Optical Materials: X 24 (2024) 100358

Contents lists available at ScienceDirect

Optical Materials: X

journal homepage: www.journals.elsevier.com/optical-materials-x

Energy transfer processes leading to strong NIR-to-red upconversion in the Yb-concentrated $Sr_3Yb_{0.98}Er_{0.02}(PO_4)_3$ eulytite

Xiaowu Hu [a], Fabio Piccinelli [a], Silvia Ruggieri [a], Pablo Camarero Linares [b,c], Patricia Haro [b,c,d], Marco Bettinelli [a,*]

[a] Luminescent Materials Laboratory, Dipartimento di Biotecnologie, University of Verona and INSTM, UdR Verona, Strada Le Grazie 15, 37134 Verona, Italy
[b] Nanomaterials for Bioimaging Group, Departamento de Física de Materiales, Facultad de Ciencias, Universidad Autónoma de Madrid, Madrid, 28049, Spain
[c] Instituto de Materiales Nicolás Cabrera, Universidad Autónoma de Madrid, Madrid, 28049, Spain
[d] Institute for Advanced Research in Chemical Sciences, Universidad Autónoma de Madrid. 28019, Madrid, Spain

ARTICLE INFO

Keywords:
Energy transfer
Upconversion
Rare earth ions
Luminescence

ABSTRACT

The optical spectroscopy and the decay kinetics of samples with composition $Sr_3Yb(PO_4)_3$, $Sr_3Y_{0.98}Yb_{0.02}(PO_4)_3$, $Sr_3Y_{0.98}Er_{0.02}(PO_4)_3$ and $Sr_3Yb_{0.98}Er_{0.02}(PO_4)_3$ have been studied at room temperature. The presence of efficient energy transfer and migration processes has been clearly evidenced in the $Sr_3Yb(PO_4)_3$ and $Sr_3Yb_{0.98}Er_{0.02}(PO_4)_3$ materials, giving rise to strong visible upconversion upon excitation in the spectral region around 1 μm in the latter material. The strong anti-Stokes emission is connected to fast migration in the $^2F_{5/2}$ level of Yb^{3+}, due to the inefficient concentration quenching for this ion. In this class of materials, the upconversion processes could be optimized even in the presence of high concentrations of the Yb^{3+} sensitizer.

1. Introduction

Eulytites constitute a family of inorganic materials having formula $A_3M(PO_4)_3$ (A = Ca, Sr, Ba; M = Y, La–Lu, Bi) and a cubic structure [1]. They are characterized by the presence of a single site for both divalent cations A and trivalent cations M, with a coordination number of 9 and a local point symmetry C_3. The shortest inter-cationic distance is distinctly short, as for A = Sr it is lower than 4 Å [2]. This has been shown to enhance the rates of energy transfer and migration processes involving trivalent lanthanide ions [2–5]. In particular, the excellent agreement between experiments and state of the art calculations [2] has clearly shown that in these materials short range interactions, such as exchange and electric quadrupole-electric quadrupole, strongly contribute to the transfer of excitation between first neighbouring cations. Due to this behaviour, in the case of $A_3Tb_{0.90}Eu_{0.10}(PO_4)_3$ (A = Sr, Ba), excitation into the $^5D_4$ level of Tb^{3+} leads to very fast and efficient migration among the Tb^{3+} subset of ions, until excitation is trapped by the $^5D_0$ level of an Eu^{3+} acceptor ion located as nearest neighbour with respect to the donor. Concentration quenching of the $^5D_4$ level is weak, as its decay time is 3.11 ms in $Sr_3La_{0.99}Tb_{0.01}(PO_4)_3$, 2.98 ms in $Sr_3Y_{0.99}Tb_{0.01}(PO_4)_3$ and 2.68 ms in $Sr_3Tb(PO_4)_3$, corresponding to a concentration quenching loss in the range 10–14 %. The overall result is a high effective $^5D_4(Tb^{3+})\rightarrow{}^5D_0(Eu^{3+})$ energy transfer efficiency (η_{ET} = 0.93 for $Sr_3Tb_{0.90}Eu_{0.10}(PO_4)_3$, 0.90 for $Sr_{1.5}Ba_{1.5}Tb_{0.90}Eu_{0.10}(PO_4)_3$ and 0.87 for $Ba_3Tb_{0.90}Eu_{0.10}(PO_4)_3$) [2].

In the field of upconversion luminescence, the most widely used lanthanide pair is the Yb^{3+}/Er^{3+} one, and anti-Stokes emission is obtained upon excitation of the $^2F_{5/2}$ level of Yb^{3+}, followed by subsequent $Yb^{3+}\rightarrow Er^{3+}$ energy transfer steps sequentially populating the green and red emitting levels of Er^{3+}, through its $^4F_{11/2}$ intermediate level [6]. To enhance the excitation rate, a relatively high concentration of Yb^{3+} is normally used (around 20 mol%) [7,8] and energy migration in the $^2F_{5/2}$ level is exploited to improve the effective energy transfer rate, by reaching a donor ion which is as close as possible to an Er^{3+} ion, which can be involved in the upconversion process. However, Yb^{3+} concentrations in the materials higher than 20 mol% are seldom used [9,10], due to the onset of concentration quenching of the luminescence [8,10,11]. This problem can be avoided by using ultrasmall monodispersed particles (such as 7–10 nm $NaYbF_4$ doped with Er^{3+} or Tm^{3+}), where presumably energy migration to quenching traps is impaired by to the small particle size [12].

The inefficient concentration quenching observed in the $^5D_4$ levels of Tb^{3+} has spurred us to study the same behaviour in the case of $Sr_3Yb(PO_4)_3$, where the $^2F_{5/2}$ level (lying around 10000 cm^{-1}) cannot be

* Corresponding author.
E-mail address: marco.bettinelli@univr.it (M. Bettinelli).

https://doi.org/10.1016/j.omx.2024.100358
Received 23 May 2024; Accepted 7 September 2024
Available online 11 September 2024

depopulated in a non-radiative way neither by cross-relaxation nor by multiphonon relaxation. This is due to the lack of intermediate levels above the ground state, and to the relatively low energy of the vibrational quanta in the eulytite lattice (980-1030 cm^{-1}) [13]. For this reason, we have found it interesting to investigate the optical spectroscopy of $Sr_3Yb(PO_4)_3$, both undoped and doped with Er, with the aim of checking if efficient upconversion can be observed in the doped material, due to efficient Yb^{3+}–Yb^{3+} and Yb^{3+}–Er^{3+} energy transfer processes occurring across short interionic distances.

In the present study we will present a detailed investigation of the various energy transfer processes occurring in undoped and Er^{3+} doped $Sr_3Yb(PO_4)_3$ leading to visible upconversion upon excitation in the Yb^{3+} energy level located in the NIR region.

2. Experimental

Eulytite samples with compositions $Sr_3Yb(PO_4)_3$ (SYb), $Sr_3Y_{0.98}Yb_{0.02}(PO_4)_3$ (SYYb), $Sr_3Y_{0.98}Er_{0.02}(PO_4)_3$ (SYEr) and $Sr_3Y_{0.98}Er_{0.02}(PO_4)_3$ (SYbEr), were prepared in polycrystalline form by solid state reaction at high temperature (1250 °C, 48 h) as previously described by some of us [1].

X-ray diffraction (XRD) patterns were collected using a Thermo ARL X'TRA powder diffractometer, in Bragg-Brentano geometry, with a Cu-anode as X-ray source and a Peltier Si (Li) cooled solid state detector with a scan rate of 1.2 °/min and an integration time of 1.5 s in the 5–90 ° 2θ range.

Luminescence spectra upon visible excitation were measured by a Fluorolog 3 (Horiba-Jobin Yvon) spectrofluorometer. The equipment was composed by a Xe lamp (450 W), a double excitation monochromator and a single emission monochromator (mod. HR320). The emitted signal was detected by means of a photomultiplier in the photon counting mode. All measurements were performed at room temperature.

For excitation in the infrared, a Ti:sapphire laser (3900S from Spectra-Physics), was used and the equipment is constituted by a monochromator (SpectraPro-500i, from Acton) and a photomultiplier tube (Hamamatsu) and an InGaAs detectors for the visible and infra-red spectral regions, respectively.

Luminescence decay curves were obtained exciting the samples with 8 ns pulses using an Optical Parametric Oscillator (OPO) pumped by a frequency tripled Nd:YAG laser (LS-2145-OPO from Lotis TII). To enhance sensitivity in NIR range, we employed a photomultiplier tube (Hamamatsu R5509-73), controlled by a high voltage power supply (Hamamatsu C9525) integrated into our system. The excitation wavelength was tuned with the assistance of a high-brightness monochromator (Shamrock 320 from Andor), while the intensity evolution over time was recorded by coupling a digital oscilloscope (LeCroy WaveRunner 6000). All measurements were performed at room temperature.

3. Results

3.1. Structural details

Undoped $Sr_3Y(PO_4)_3$ and $Sr_3Yb(PO_4)_3$ eulytites crystallize in the cubic space group $I\bar{4}3d$ (number 220). (PDF card 00-044-0320 and PDF card 00-048-0409, respectively), with almost the same cell volume (1033.29 and 1028.59 $Å^3$, respectively). The Sr^{2+}/M^{3+} pairs of cations are disordered on a single crystallographic site, whilst the oxygen atoms of the phosphate groups are distributed over three partially occupied sites [1]. The Y^{3+} and Yb^{3+} ions, and the Er^{3+} dopants are accommodated in the single disordered cationic site 16c having C_3 point group symmetry.

XRD experiments confirmed that all the obtained materials are single phase with a eulytite-type structure (Fig. 1).

As expected, the cell parameters determined from XRPD data, are only slightly affected by the nature of trivalent cation. In particular, the cell volumes are within the range of 1028.59 $Å^3$ [for $Sr_3Yb(PO_4)_3$] - 1033.29 $Å^3$ [for $Sr_3Y(PO_4)_3$], as reported in Table 1.

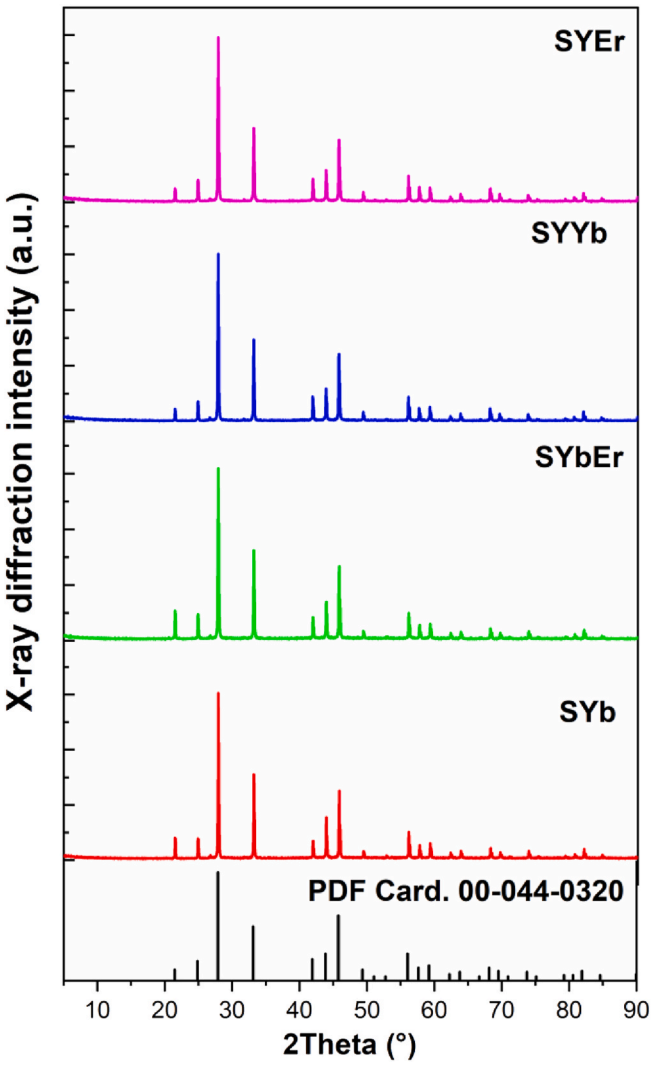

Fig. 1. X-ray powder diffraction (XRPD) patterns of the samples under investigation. The PDF card 00-044-0320 of $Sr_3Y(PO_4)_3$ is also reported.

3.2. Luminescence spectroscopy

3.2.1. Yb^{3+}-based materials

The energy level structure of the Yb^{3+} and Er^{3+} ions investigated in this study is presented in Fig. 2.

The excitation and emission spectra of SYYb and SYb are shown in

Table 1
Crystallographic cell parameters of the samples under investigation.

Sample	Cell parameters	
	a (Å)	Volume ($Å^3$)
$Sr_3Yb(PO_4)_3$	10.094[a]	1028.59[a]
SYb	10.098(1)	1029.7(1)
SYbEr	10.105(1)	1031.8(1)
SYYb	10.108(1)	1032.8(1)
SYEr	10.110(1)	1033.3(1)
$Sr_3Y(PO_4)_3$	10.110[b]	1033.29[b]

[a] PDF card 00-048-0409.
[b] PDF card 00-044-0320.

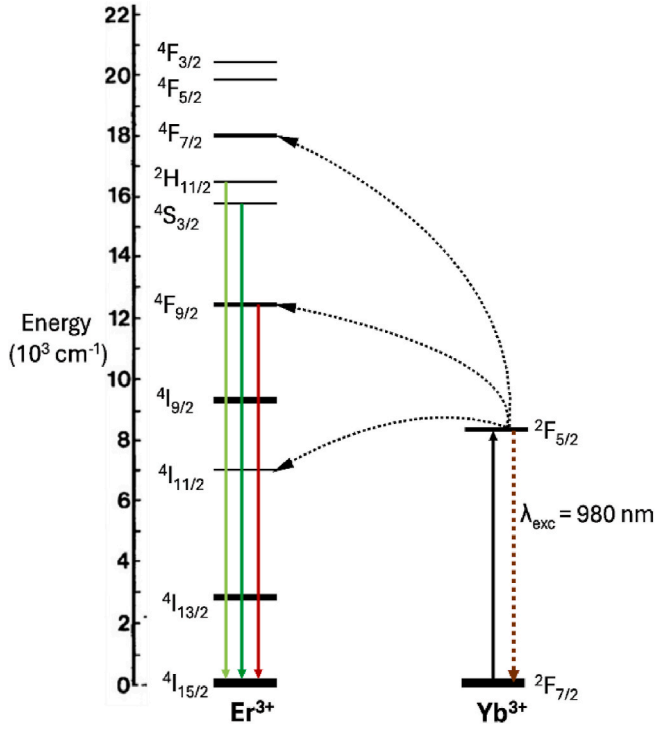

Fig. 2. Energy level structure of the Yb^{3+} and Er^{3+} ions showing the levels involved in the upconversion process and the ones responsible for the red and green emission of Er^{3+}. (For interpretation of the references to colour in this figure legend, the reader is referred to the Web version of this article.)

Fig. 3, together with a schematic energy level diagram for the $^2F_{7/2}$ and $^2F_{5/2}$ multiplets of the Yb^{3+} ion (Fig. 4). The spectra, obtained upon emission and excitation in the NIR region, show the well-known $^2F_{7/2}\leftrightarrow{}^2F_{5/2}$ transitions around 1 μm.

The decay curves of the $^2F_{5/2}$ level of Yb^{3+} in SYYb and concentrated SYb are shown in Fig. 5.

They are perfectly exponential with decay times of 1.370 and 0.440 ms, respectively. These values imply that the quenching loss in concentrated SYb, presumably due to migration and transfer to killer centres, is of the order of 68 %, *i.e.* a quenching efficiency equal to 0.68. This value is significantly higher than for $Sr_3Tb(PO_4)_3$ with respect to $Sr_3Y_{0.99}Tb_{0.01}(PO_4)_3$ (10 %) [5], but for the concentrated material the luminescence of Yb^{3+} is still very strong. The perfectly exponential decay presumably indicates that the transfer to the killer centres is preceded by a very fast migration process, in qualitative agreement with what observed in the case of $Sr_3Tb(PO_4)_3$ and $Ba_3Tb(PO_4)_3$ [2,5]. However, we point out that in materials containing high amounts of Yb^{3+} self-quenching processes more complicated than energy migration to unwanted impurities may occur, as shown by Auzel et al. [14]. This could at least partly explain the stronger quenching of the Yb^{3+} emission in $Sr_3Yb(PO_4)_3$, compared to $Sr_3Tb(PO_4)_3$ and $Ba_3Tb(PO_4)_3$.

3.2.2. *Er^{3+}-based materials*

The room temperature emission spectrum of SYEr in the visible region, obtained upon excitation at 378 nm (not shown), is, as it is usual, dominated by the green ($^2H_{11/2}$, $^4S_{3/2}$)→$^4I_{15/2}$ transition, whilst the $^4F_{9/2}\rightarrow{}^4I_{9/2}$ transition is distinctly weaker. The excitation spectrum (not shown) of the emission at 545 nm from ($^2H_{11/2}$, $^4S_{3/2}$) is dominated by the hypersensitive transition $^4I_{15/2}\rightarrow{}^4G_{11/2}$ located in the UV region. The Er^{3+} spectra are similar to many other data reported in the literature (see for example [15]). The decay curves of the luminescence from both ($^2H_{11/2}$, $^4S_{3/2}$) and $^4F_{9/2}$, upon excitation at 378 nm, are slightly non-exponential with effective decay times which are very similar, both close to 17 μs. This behaviour is presumably explained by the fact that the upper level is the main feeding state of the lower [16].

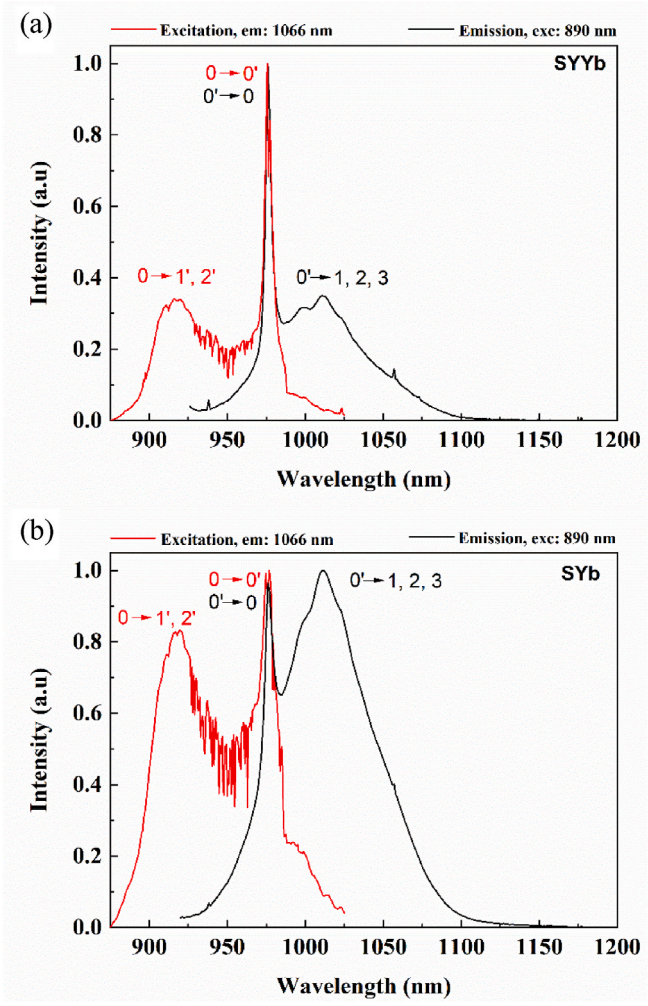

Fig. 3. Room temperature excitation (red line) and emission (black line) spectra of (a) SYYb and (b) SYb samples. (For interpretation of the references to colour in this figure legend, the reader is referred to the Web version of this article.)

The emission spectrum of the same material in the NIR (1400–1700 nm), obtained at room temperature upon excitation at 890 nm in the $^4I_{11/2}$ level (Fig. 6) is composed of a strong and structured band peaking close to 1550 nm. This feature is assigned to the transition from $^4I_{13/2}$ to the ground state $^4I_{15/2}$. The upper lying state is populated through multiphonon relaxation from $^4I_{11/2}$ to the lower lying $^4I_{13/2}$ as their energy gap is about 3800 cm^{-1}, and in eulytites it can be spanned by less than four vibrational quanta due to P–O stretching modes [13]. The excitation spectrum measured with observation at 1066 nm shows a strong band peaking at extending from 890 to 1050 nm, assigned to the $^4I_{15/2}\rightarrow{}^4I_{11/2}$ transition of Er^{3+}.

The decay profile of the $^4I_{11/2}$ level in SYEr, obtained with $\lambda_{exc} = 920$ and $\lambda_{obs} = 1020$ nm, is shown in Fig. 7. The curve is exponential, as expected for isolated Er^{3+} centres, with a decay constant of 0.217 ms.

3.2.3. *Yb^{3+}-Er^{3+}-based materials*

The anti-Stokes emission spectra of SYbEr, obtained upon laser excitation in the region close to 1 μm, where both Er^{3+} and Yb^{3+} absorb radiation, are shown in Fig. 8.

The spectra are composed of two Er^{3+} transitions located in the visible region, *i.e.* ($^2H_{11/2}$, $^4S_{3/2}$)→$^4I_{15/2}$, and $^4F_{9/2}\rightarrow{}^4I_{15/2}$. The relative intensity of the $^4F_{9/2}\rightarrow{}^4I_{15/2}$ band slightly increases when the excitation moves from 975 to 920 nm. These data show that in the present eulytite

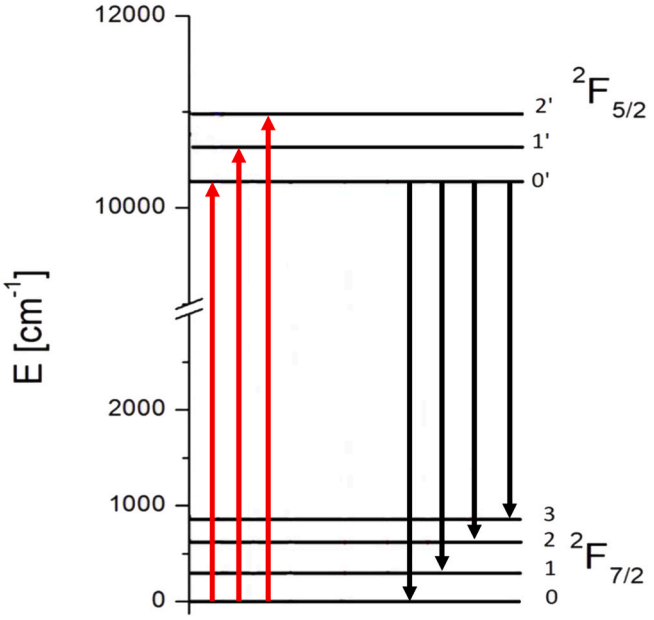

Fig. 4. Schematic energy diagram of the Stark (crystal field) levels of the Yb^{3+} ion.

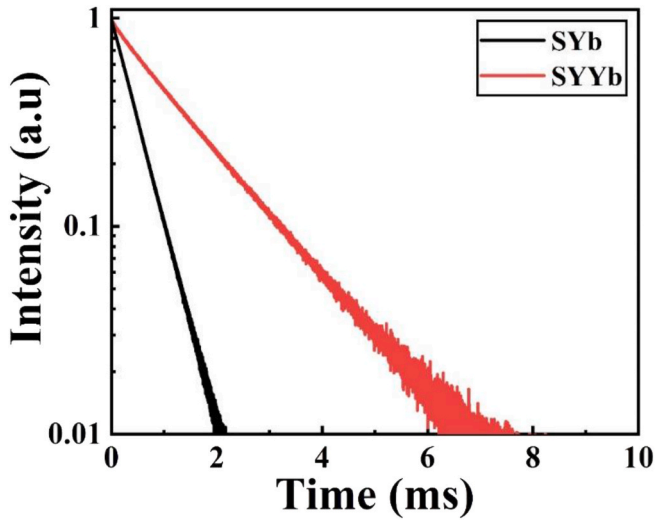

Fig. 5. Room temperature $^2F_{5/2}$ decay curves of Yb^{3+} in SYYb (red line) and SYb (black line). λ_{exc} = 920 nm; λ_{em} = 1020 nm. (For interpretation of the references to colour in this figure legend, the reader is referred to the Web version of this article.)

host the upconversion deriving from the Yb^{3+}/Er^{3+} is strong.

The excitation spectra measured with λ_{obs} = 545 and 658 nm, *i.e.* in the ($^2H_{11/2}$, $^4S_{3/2}$)→$^4I_{15/2}$ and $^4F_{9/2}$ → $^4I_{15/2}$ transitions, are composed of two bands (Fig. 9) that can be ascribed to the $^2F_{7/2}$→$^2F_{5/2}$ transition of Yb^{3+} (see the spectra shown above for the SYb sample). This clearly indicates that excitation in the NIR predominantly populates the $^2F_{5/2}$ level of Yb^{3+}, that acts as a sensitizer in the upconversion process, due to its high concentration with respect to Er^{3+}.

In the case of SYbEr, the decay profile of the NIR emission, obtained upon pulsed excitation at 920 nm, *i.e.* in the $^2F_{5/2}$ and $^4I_{11/2}$ levels, is characterized by a fast buildup at short times (about 13 μs), followed by an exponential decay with a decay constant close to 109 μs (Fig. 10).

Based on the energy level diagram, the two energy levels are quasi-resonant, and therefore the analysis of the decay profiles is not trivial. We propose that the risetime is associated with the kinetics relative to

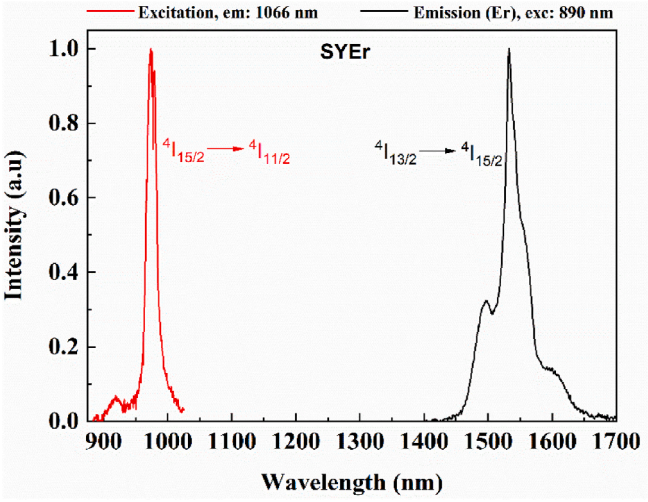

Fig. 6. Room temperature excitation (red line) and emission (black line) spectra of SYEr. (For interpretation of the references to colour in this figure legend, the reader is referred to the Web version of this article.)

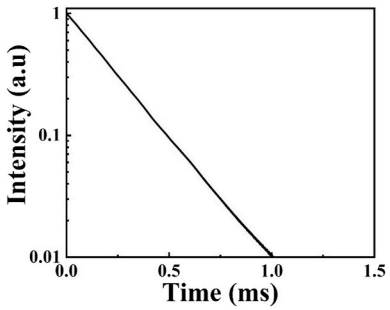

Fig. 7. Room temperature $^4I_{11/2}$ decay curve of the NIR emission of Er^{3+} in SYEr. λ_{exc} = 920 nm; λ_{em} = 1020 nm.

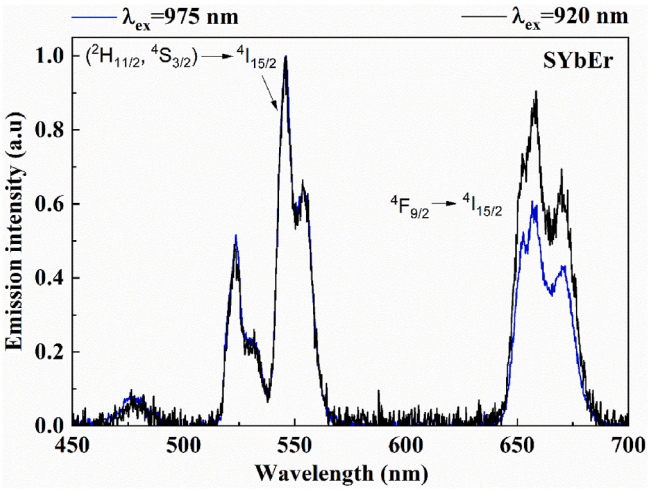

Fig. 8. Room temperature anti-Stokes emission spectra of SYbEr upon excitation at two different wavelengths (λ_{exc} = 920 nm; black line and λ_{exc} = 975 nm; blue line). (For interpretation of the references to colour in this figure legend, the reader is referred to the Web version of this article.)

the faster decaying $^4I_{11/2}$ level of the Er^{3+} ion, which is fed by the slower decaying $^2F_{5/2}$ level of the Yb^{3+} ion, responsible for the absorption of most of the photons [17,18]. This assumption is supported by the fact that $^4I_{11/2}$ is also depopulated by the upward transition associated with

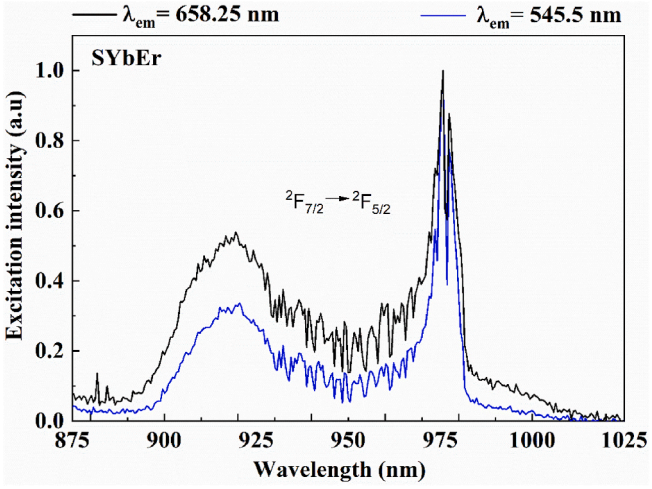

Fig. 9. Room temperature excitation spectra of SYbEr recorded at two different wavelengths (λ_{em} = 658.25 nm; black line and λ_{em} = 545.5 nm; blue line). (For interpretation of the references to colour in this figure legend, the reader is referred to the Web version of this article.)

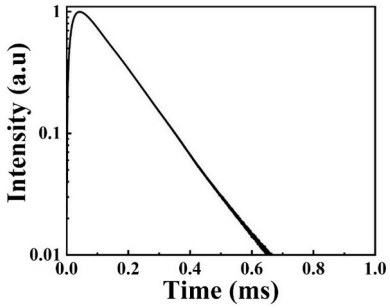

Fig. 10. Room temperature decay curve of the NIR luminescence of the SYbEr sample. (λ_{exc} = 920 nm; λ_{em} = 1020 nm).

the upconversion process. According to this reasoning, we assign to the decay time of the Yb^{3+} ion, in the Er^{3+} containing material, the value 100 μs. This value gives rise to an energy transfer efficiency η_T, evaluated using the following equation, where τ_{Yb-Er} and τ_{Yb} are the decay times of Yb^{3+} in the presence and in the absence of Er^{3+}, respectively,

$$\eta_T = 1\text{-}\tau_{Yb-Er}/\tau_{Yb} \quad (1)$$

having a value of 0.75. This transfer efficiency is ultimately responsible for the upconversion process; it must be regarded as very high, and accounts for the strong anti-Stokes emission observed for the material under investigation.

4. Discussion

The high efficiency estimated for the energy transfer process leading to upconversion in SYbEr appears to be promising for possible applications. However, in order to fully evaluate the potential of the present approach to upconversion, a more detailed discussion is necessary.

The overall efficiency of the processes leading to upconversion (η_{tot}) can be approximately calculated using the following equation

$$\eta_{tot} = (1\text{-}\eta_{quench}) \times \eta_T \times c_{Yb} \quad (2)$$

where η_{quench} is the quenching efficiency (0.68, see above) and therefore $(1\text{-}\eta_{quench})$ is the energy migration efficiency in the Yb^{3+} subset of ions (0.32), η_T is the energy transfer efficiency between Yb^{3+} and Er^{3+} (0.75) and c_{Yb} is the fraction of the Yb^{3+} present in formula (0.98), and therefore responsible for the sensitization of the upconversion. This calculation yields the value $\eta_{tot} \approx 0.24$. The calculation is only approximate, as other loss mechanisms should have been considered. Among them, the most important one is the multiphonon relaxation from $^4I_{11/2}$ to $^4I_{13/2}$. This process has been studied before [19,20], but in order to obtain the nonradiative decay rate, the knowledge of the radiative lifetime of the $^4I_{11/2}$ level is required. This value could be obtained on the basis of the absorption spectra through a Judd-Ofelt calculation, but unfortunately these data are difficult to obtain for powder eulytite samples, in the absence of suitable single crystals. Another possibility would be the experimental measurement of the quantum efficiency of the luminescence originating from $^4I_{11/2}$ of Er^{3+}, but this measurement unfortunately lies beyond the experimental facilities of our laboratories. Despite the lack of this information, the present calculation appears to yield a reasonably high value, taking into account that the material under investigation is almost fully concentrated (98 %) in the Yb^{3+} ions that are responsible for the absorption of photons.

On the other hand, in the fluoride materials currently used to generate upconversion, the concentration of Yb^{3+} is normally lower than 20 mol% [9,10], so that $c_{Yb} \leq 0.20$. This lower concentration of Yb^{3+} gives rise to values of η_{tot} being in principle five times lower than the one reported here. Another feature of the materials described here is that fast energy migration brings rapidly the excitation in the proximity of the Er^{3+} ions, so that the energy transfer rate is maximized. On the contrary, in fluoride materials where $c_{Yb} \leq 0.20$ the average distances between Yb^{3+} and Er^{3+} are longer, so that the $Yb^{3+} \rightarrow Er^{3+}$ energy transfer is bound to be less probable. Finally, the oxide materials described here are much less prone to the contamination by quenching impurities than the fluoride ones normally presented in the literature [21], and their synthesis does not require the use of hazardous fluoride-based reagents.

5. Conclusions

In the present paper we have presented a detailed study of the optical spectroscopy and excited state dynamics of the eulytite materials with compositions $Sr_3Y_{0.98}Yb_{0.02}(PO_4)_3$, $Sr_3Y_{0.98}Er_{0.02}(PO_4)_3$, $Sr_3Yb(PO_4)_3$ and $Sr_3Yb_{0.98}Er_{0.02}(PO_4)_3$. In particular, we have concentrated our attention on the Yb^{3+}–Yb^{3+} and Yb^{3+}–Er^{3+} energy transfer processes leading to upconversion from NIR excitation to emission located in the green and red spectral regions. We have shown that fast energy migration in the Yb^{3+} subset of ions leads to the efficient population of the Er^{3+} energy levels that give rise to anti-Stokes emission. The overall efficiency of the upconversion process has been estimated, and a promising, but approximate, value of 0.24 has been obtained. The materials under investigation could hold some promise for future applications in the field of upconversion phosphors. However, we must point out that upconverting materials are particularly important when obtained as isolated and well-defined particles of nanometric size, and that eulylite materials have not been synthesized in this form yet, to the best of our knowledge. This could be tricky, since oxide nanomaterials are prone to aggregation, and isolated particles could be hard to obtain. In any case, the present study could be useful, in order to develop new schemes to improve upconversion research.

CRediT authorship contribution statement

Xiaowu Hu: Investigation. **Fabio Piccinelli:** Investigation, Writing – review & editing. **Silvia Ruggieri:** Investigation, Writing – review & editing. **Pablo Camarero Linares:** Investigation, Validation. **Patricia Haro:** Investigation, Validation. **Marco Bettinelli:** Formal analysis, Investigation, Methodology, Writing – original draft.

Declaration of competing interest

The authors declare that they have no known competing financial interests or personal relationships that could have appeared to influence the work reported in this paper.

Data availability

Data will be made available on request.

Acknowledgments

The authors gratefully thank Erica Viviani (Univ. Verona) for expert technical assistance and the Facility "Centro Piattaforme Tecnologiche" of the University of Verona for the access to the Fluorolog 3 (Horiba-Jobin Yvon) spectrofluorometer and Thermo ARL X'TRA powder diffractometer. Funding from the University of Verona (FUR scheme) is gratefully acknowledged. X. W. was financially supported by the China Scholarship Council (CSC) No.201906130187 for a 3-years period in Italy as a PhD. Student. The authors would like to acknowledge Prof. Marta Quintanilla Morales and Prof. Eugenio Cantelar Alcalde (Univ. Autónoma de Madrid) for expert technical support during luminescence measurement with Ti:sapphire equipment. Besides, this work was financed by Grant TED2021-129937B–I00, CNS2022-135495, and PID2023-151078OB-I00 funded by MCIN/AEI/10.13039/501100011033 and by the European Union NextGenerationEU/PRTR. P. Camarero acknowledges Programa Investigo (Plan de Recuperación, Transformación y Resiliencia) which was developed thanks to SEPE, Ministerio de Trabajo y Economía Social and the European Union through NextGenerationEU.

References

[1] J. Barbier, Structural refinements of eulytite-type $Ca_3Bi(PO_4)_3$ and $Ba_3La(PO_4)_3$, J. Solid State Chem. 101 (1992) 249–256, https://doi.org/10.1016/0022-4596(92)90181-T.

[2] A.N. Carneiro Neto, R.T. Moura, A. Shyichuk, V. Paterlini, F. Piccinelli, M. Bettinelli, O.L. Malta, Theoretical and experimental investigation of the Tb→Eu energy transfer mechanisms in cubic $A_3Tb_{0.90}Eu_{0.10}(PO_4)_3$ (A = Sr, Ba) materials, J. Phys. Chem. C 124 (2020) 10105–10116, https://doi.org/10.1021/acs.jpcc.0c00759.

[3] M. Bettinelli, A. Speghini, F. Piccinelli, J. Ueda, S. Tanabe, Energy transfer processes in $Sr_3Tb_{0.90}Eu_{0.10}(PO_4)_3$, Opt. Mater. 33 (2010) 119–122, https://doi.org/10.1016/j.optmat.2010.07.008.

[4] M. Bettinelli, F. Piccinelli, A. Speghini, J. Ueda, S. Tanabe, Excited state dynamics and energy transfer rates in $Sr_3Tb_{0.90}Eu_{0.10}(PO_4)_3$, J. Lumin. 132 (2012) 27–29, https://doi.org/10.1016/j.jlumin.2011.07.018.

[5] V. Paterlini, F. Piccinelli, M. Bettinelli, Tb→Eu energy transfer processes in eulytite $A_3Tb(PO_4)_3$ (A=Sr, Ba) and silico-carnotite $Ca_3Tb_2Z_3O_{12}$ (Z=Si, Ge) materials doped with Eu, Phys. B Condens. Matter 575 (2019) 411685, https://doi.org/10.1016/j.physb.2019.411685.

[6] F. Auzel, Upconversion and anti-Stokes processes with f and d ions in solids, Chem. Rev. 104 (2004) 139–174, https://doi.org/10.1021/cr020357g.

[7] F. Wang, X. Liu, Upconversion multicolor fine-tuning: visible to near-infrared emission from lanthanide-doped $NaYF_4$ nanoparticles, J. Am. Chem. Soc. 130 (2008) 5642–5643, https://doi.org/10.1021/ja800868a.

[8] S. Heer, K. Kömpe, H.-U. Güdel, M. Haase, Highly efficient multicolour upconversion emission in transparent colloids of lanthanide-doped $NaYF_4$ nanocrystals, Adv. Mater. 16 (2004) 2102–2105, https://doi.org/10.1002/adma.200400772.

[9] Q. Zhan, J. Qian, H. Liang, G. Somesfalean, D. Wang, S. He, Z. Zhang, S. Andersson-Engels, Using 915 nm laser excited Tm/Er/Ho-doped $NaYbF_4$ upconversion nanoparticles for in vitro and deeper in vivo bioimaging without overheating irradiation, ACS Nano 5 (2011) 3744–3757, https://doi.org/10.1021/nn200110j.

[10] P. Du, L. Luo, J.S. Yu, Upconversion emission and cathodoluminescence of Er-doped $NaYbF_4$ nanoparticles for low-temperature thermometry and field emission displays, Appl. Phys. 123 (2017) 157, https://doi.org/10.1007/s00339-016-0744-x.

[11] W.Q. Santos, A.S.S. de Camargo, D. Wu, W.F. Silva, L. Zhang, C. Jacinto, Cooperative upconversion, radiation trapping, and self-quenching effects in highly Yb-doped oxyfluoride glasses, Sci. Adv. Mater. 5 (2013) 1948–1953, https://doi.org/10.1166/sam.2013.1661.

[12] G. Chen, T.Y. Ohulchanskyy, R. Kumar, H. Ågren, P.N. Prasad, Ultrasmall monodisperse NaYF4:Yb/Tm nanocrystals with enhanced near-infrared to near-infrared upconversion photoluminescence, ACS Nano 4 (2010) 3163–3168, https://doi.org/10.1021/nn100457j.

[13] Q. Chen, Y. Hao, Q. Chen, Eu^{2+} activated novel eulytite $Na_3Bi_5(PO_4)_6$:Eu phosphors: enhanced luminescence and thermal stability for photonics application, Ceram. Int. 48 (2022) 15165–15179, https://doi.org/10.1016/j.ceramint.2022.02.046.

[14] F. Auzel, G. Baldacchini, L. Laversenne, G. Boulon, Radiation trapping and self-quenching analysis in Yb, Er, and Ho doped Y_2O_3, Opt. Mater. 24 (2003) 103–109, https://doi.org/10.1016/S0925-3467(03)00112-5.

[15] J.A. Capobianco, P. Kabro, F.S. Ermeneux, R. Moncorgé, M. Bettinelli, E. Cavalli, Optical spectroscopy, fluorescence dynamics and crystal-field analysis of Er^{3+} in YVO_4, Chem. Phys. 214 (1997) 329–340, https://doi.org/10.1016/S0301-0104(96)00318-7.

[16] P. Kabro, J.A. Capobianco, F.S. Ermeneux, R. Moncorgé, M. Bettinelli, E. Cavalli, Excited state dynamics and energy transfer processes in YVO4:Er crystals, J. Appl. Phys. 82 (1997) 3983–3986, https://doi.org/10.1063/1.365706.

[17] J.F. Suyver, J. Grimm, K.W. Krämer, H.U. Güdel, Highly efficient near-infrared to visible up-conversion process in $NaYF_4$:Er^{3+},Yb^{3+}, J. Lumin. 114 (2005) 53–59, https://doi.org/10.1016/j.jlumin.2004.11.012.

[18] M.T. Berry, P.S. May, Disputed mechanism for NIR-to-red upconversion luminescence in $NaYF_4$:Yb^{3+},Er^{3+}, J. Phys. Chem. A 119 (2015) 9805–9811, https://doi.org/10.1021/acs.jpca.5b08324.

[19] C.B. Layne, W.H. Lowdermilk, M.J. Weber, Multiphonon relaxation of rare-earth ions in oxide glasses, Phys. Rev. B 16 (1977) 10–20, https://doi.org/10.1103/PhysRevB.16.10.

[20] R. Reisfeld, Y. Eckstein, Radiative and non-radiative transition probabilities and quantum yields for excited states of Er^{3+} in germanate and tellurite glasses, J. Non-Cryst. Solids 15 (1974) 125–140, https://doi.org/10.1016/0022-3093(74)90117-3.

[21] K.W. Krämer, D. Biner, G. Frei, H.U. Güdel, M.P. Hehlen, S.R. Lüthi, Hexagonal sodium yttrium fluoride based green and blue emitting upconversion phosphors, Chem. Mater. 16 (2004) 1244–1251, https://doi.org/10.1021/cm031124o.